An attenuating mutation in a neurovirulent Sindbis virus strain interacts with the IPS-1 signaling pathway in vivo

Amy C. Wollish[1,2,3], **Martin Ferris**[1,2,3], **Lance Blevins**[1,2,3], **Yueh-Ming Loo**[4], **Michael Gale Jr**[4], and **Mark T. Heise**[1,2,3,*]

[1]Department of Genetics, University of North Carolina at Chapel Hill, Chapel Hill, North Carolina 27599

[2]Department of Microbiology and Immunology, University of North Carolina at Chapel Hill, Chapel Hill, North Carolina 27599

[3]The Carolina Vaccine Institute, University of North Carolina at Chapel Hill, Chapel Hill, North Carolina 27599

[4]Department of Immunology, University of Washington School of Medicine, Seattle, WA 98195 7650.

Introduction

Sindbis virus (SINV) is the prototypic member of the alphavirus genus, and provides an excellent model of viral induced encephalomyelitis in mice. The SINV model has been used to define the immune processes required for recovery and viral clearance from neurons (reviewed in (Griffin, 2010)). Survival of mice infected with SINV is dependent on a number of factors, including viral genetics, host age, and interactions with the host innate and adaptive immune pathways (Dropulic et al., 1997, Griffin et al., 1994, Heise et al., 2000, Johnson et al., 1972, Kobiler et al., 1999, Labrada et al., 2002, Park and Griffin, 2009, Ryman et al., 2000, Tucker et al., 1993, Tucker et al., 1997).

Among multiple SINV virus strains in the literature, wild type AR86 (hereafter S300) and neuro-adapted NSV are among the few SINVs that maintain the ability to cause lethal neurologic disease in adult mice (Simpson et al., 1996, WEINBREN et al., 1956). AR86 and NSV were independently derived strains, and while immune pathology plays a major role during NSV infection, studies suggest that the immune system is protective during AR86 infection. Previous studies with S300 identified four viral genetic determinants of adult neurovirulence in outbred CD 1 mice, three of which were in the nonstructural proteins (Suthar et al., 2005). One of these determinants, a threonine (Thr) codon at nsP1 position 538, is essential for S300 neurovirulence, where an attenuating isoleucine (Ile, consensus among non neurovirulent SINV viruses) at this position accelerates polyprotein processing and expression from the 26S RNA promoter (Heise et al., 2003). S300 expressing this Ile (referred to as nsP1 T538I hereafter), has no defect in its ability to establish infection within

---

Corresponding author: Mark T. Heise, PhD, The Carolina Vaccine Institute, University of North Carolina at Chapel Hill, 9039 Burnett Womack Bldg., CB #7292, Chapel Hill, NC 27599, Tel: (919) 843 1492, Fax: (919) 843 6924, heisem@med.unc.edu.

Conflict of Interest Statement. The authors report no conflict of interest.

the CNS through 4 days post-infection (dpi), even exhibiting increased early replication as compared to S300. However, in CD-1 mice, nsP1 T538I viral RNA within the brain was dramatically reduced at late times pi (Heise et al., 2000).

Type I interferon (interferon alpha/beta [IFN-α/β]) is critical for host survival upon infection with alphaviruses (Ryman et al., 2000, White et al., 2001). Indeed, SINV is highly sensitive to the antiviral effects of IFN-α/β (Yin et al., 2009) and *in vitro* data suggest that SINV antagonizes IFN-α/β induction via global shutoff of host macromolecular synthesis (Burke et al., 2009, Frolova et al., 2002). Differences in host shutoff do not explain the attenuation of the nsP1 T538I virus. Importantly, the nsP1 T538I virus shuts off host macromolecular synthesis equivalently to S300, nsP1 T538I fails to antagonize early type I or II IFN-dependent signaling at or prior to STAT phosphorylation (Cruz et al., 2010, Simmons et al., 2010), suggesting that this determinant affects neurovirulence via specific interactions with the IFN pathway.

The type I IFN response to RNA viruses is initiated by the ligation of 'foreign' pattern associated molecular patterns (PAMPs) to specific Pattern Recognition Receptors (PRRs), which include the Toll like receptors (TLRs) and RIG-I-like receptors (RLRs) (Janeway, 1989, Uematsu and Akira, 2006). The TLR family is comprised of 12 known murine transmembrane receptors (human TLR8 functions analogously to murine TLR7), including four that are known to recognize RNA virus PAMPs (TLR 2, -3, -4, -7, and -8) (Akira, 2003, Brennan and Bowie, 2010, Colonna, 2007, Matsumoto et al., 2011, Uematsu and Akira, 2006, Yokota et al., 2010). TLRs are type I transmembrane proteins that contain extracellular leucine-rich repeats (LRRs), required to detect PAMPs, and a cytoplasmic Toll/ interleukin 1 receptor (TIR) domain, required for activation of downstream signaling pathways. TLR3 and TLR7/8 are localized to intracellular vesicles, where they recognize viral double stranded (ds) RNA and single stranded RNA, respectively (Diebold et al., 2004, Lund et al., 2004, Matsumoto et al., 2004). TLR2 and TLR4 are localized to the cell surface, where they recognize viral structural proteins, along with bacterial PAMPs (reviewed in (Kawai and Akira, 2007)). MyD88 is the essential adaptor protein required for TLR signaling through all of the TLRs, except for TLR3 and the MyD88-independent pathway of TLR4 signaling, both of which can signal via the adaptor Toll/IL-1R domain containing adaptor inducing IFN-β (TRIF, also known as Ticam-1) (Colonna, 2007, Kawai and Akira, 2007, Kawai and Akira, 2011, Matsumoto et al., 2011, Oshiumi et al., 2003, Sasai et al., 2010, Yamamoto et al., 2003).

The RLRs: melanoma differentiation associated gene (Mda)5 and retinoic acid inducible gene (RIG)-I, are localized to the cytoplasm where they recognize specific RNA motifs within viral RNA, such as 5' triphosphates on uncapped RNA and dsRNA (Hornung et al., 2006, Kato et al., 2006, Kato et al., 2008, Loo et al., 2008, Pichlmair et al., 2006). Once activated, the RLRs undergo a conformational change that allows them to bind via a caspase recruitment domain (CARD) to Interferon promoter stimulator (IPS)-1 (also known as Cardif, Visa, and MAVS), which is located on mitochondria associated membranes (Horner et al., 2011, Kumar et al., 2006).

The ligation of PRRs results in the activation of latent transcription factors, interferon regulatory factor (IRF)-3, IRF-7, and NF-κB, which in turn induce IFN, hundreds of interferon-stimulated genes (ISGs), along with inflammatory cytokines (reviewed in (Colonna, 2007, Hiscott, 2007)). To date, a number of specific anti SINV ISGs have been identified, including the ubiquitin like ISG15, Viperin, ISG12, ISG20, ZAP, dsRNA dependent protein kinase (PKR) (Bick et al., 2003, Giannakopoulos et al., 2009, Lenschow et al., 2005, Lenschow et al., 2005, Lenschow et al., 2007, MacDonald et al., 2007, Ryman et al., 2005, Zhang et al., 2007). PKR is unique amongst these in that it is also a PRR,

recognizing short stem loops within RNA in an RLR-independent manner. Upon activation, PKR activates IRF-3 and induces the phosphorylation of eIF2α, which inhibits host and certain viral translation and activates the host stress response (Nallagatla et al., 2007).

Much emphasis has been placed on understanding which host PRRs recognize alphavirus PAMPs and which PRRs mediate IFN-α/β production. As such, Esen et al. demonstrated that neither MyD88 nor TLR3 modulated mouse neurovirulence of SINV strain NSV (Esen et al., 2012, Kim et al., 2008, Tabeta et al., 2006). In primary murine fibroblast cells, type I IFN induction by SINV was shown to be largely dependent on PKR and Mda5 (Burke et al., 2009), however Mda5 was not required for SINV-induced IFN-α production in primary bone-marrow derived macrophages (Gitlin et al., 2006). Recently, IPS-1 was shown to be critical for activation of IRF3 and IFN-α/β production within fibroblasts after infection with a related alphavirus, chikungunya virus (CHIKV) (White et al., 2010). However, IPS-1 deficient mice were only slightly more susceptible to CHIKV peripheral infection, and exhibited increased CHIKV replication in the serum at 48 hours pi, but not in other organs or at other time-points (Schilte et al., 2010) A study with West Nile virus demonstrated that IPS-1 is essential for the regulated activation of the innate and adaptive immune responses (Suthar et al., 2010).

Given that the nsP1 T538I virulence determinant modulates IFN-α/β induction, we set out to determine whether viral interactions with specific IFN-α/β induction pathways were important for regulating viral neurovirulence. To define the pathway(s) of innate immune activation by nsP1 T538I, as well as the wild type S300 virus, we directly compared S300 to nsP1 T538I i. c. infection in mice on the C57BL/6J background deficient for IFN-α/β / receptor (IFN-α/βR), MyD88, TRIF, and IPS-1. The studies herein demonstrate that in the complete absence of IFN-α/β signaling, the attenuated virus regains virulence comparable to S300, and both viruses show markedly increased virulence. This result suggests that the AR86 strain of SINV interacts with the type I IFN system to regulate virulence *in vivo*. We find that the IPS-1 signaling pathway plays a major role in controlling the attenuated nsP1 T538I virus and limiting SINV-induced morbidity and mortality. Furthermore, we demonstrate that while the TLR pathways are dispensable for nsP1 T538I replication control, TLR signaling via the TRIF adaptor molecule and not MyD88 may modulate the neurovirulence of SINV.

Results

A threonine at nsP1 position 538 is a critical determinant of SINV neurovirulence

The S300 strain of SINV is highly neurovirulent in adult mice, (Heise et al., 2000, Simpson et al., 1996) and we have previously identified four viral genetic determinants that regulate neurovirulence (Suthar et al., 2005). One of these determinants, a Thr codon at nsP1 position 538, is essential for S300 neurovirulence, where an attenuating Ile at this position decreases viral neurovirulence without adversely affecting viral replication *in vitro* or the ability of the virus to establish infection within the CNS (Heise et al., 2000). Previous studies with this attenuated mutant were conducted in outbred CD-1 mice. However, to further analyze how this virus interacts with the host immune response, we confirmed that the nsP1 T538I mutant exhibits an attenuated phenotype after infection of inbred C57BL/6J mice. As shown in Fig. 1A, infection of female adult C57BL/6J mice with S300 resulted in 100% lethality with a mean survival time (MST) of 6.3 days (n=49) post i.c. inoculation. Infection with nsP1 T538I resulted in 62. 5% mortality and an increased MST of 10.7 dpi (n=56) (Fig. 1A and Table 1,2). Moreover, S300 infected C57BL/6J mice displayed enhanced weight loss from 4–7 dpi as compared to nsP1 T538I infected mice. C57BL/6J mice infected with nsP1 T538I began to regain weight beginning on day 9 pi, while S300 infected mice never showed signs of weight gain/recovery (Fig. 1B, Table 3). Therefore, although the attenuated mutant

caused more severe disease in the C57BL/6J background than was previously reported in outbred CD-1 mice, the mutant virus is still significantly attenuated in C57BL/6J mice when compared to S300 virus (Fig. 1). Further analysis indicated that the nsP1 T538I virus replicated equivalently to S300 virus at 1 and 3 dpi within the CNS, however nsP1 T538I titers were significantly reduced as compared to S300 in the brain on 5 and 6 dpi, and in the spinal cord on day 6 pi (Fig. 1C and D). These results suggest that the nsP1 538 virus is able to efficiently establish infection within the CNS, but that the virus is likely cleared more efficiently than S300.

The nsP1 T538I displays comparable virulence to S300 in the absence of a functional type-I IFN system

We have previously demonstrated that nsP1 T538I induces higher amounts of IFN-α/β compared to S300 in the serum of infected CD-1 and C57BL/6J mice and in cell culture (Cruz et al., 2010). Therefore, to evaluate whether the mutant virus would regain wild type virulence in the absence of IFN-α/β signaling we infected IFN-α/βR deficient mice with either S300 or nsP1 T538I and assessed neurovirulence. Consistent with previous studies (Ryman et al., 2000), IFN-α/β / R$^{-/-}$ mice were highly susceptible to infection with SINV, and exhibited rapid and equivalent mortality and weight loss upon infection with either S300 or nsP1 T538I viruses (Fig. 2A and B). Specifically, infection of IFN-α/βR$^{-/-}$ mice with either S300 or nsP1 T538I resulted in 100% mortality and an MST of 3.5 and 3.4 dpi for S300 and nsP1 T538I, respectively. (Fig. 2A, Table 1, 2). Furthermore, both S300 and nsP1 T538I replicated approximately 3 logs higher within the brain and spinal cord of IFN-α/β/R$^{-/-}$ mice as compared to C57BL/6J mice on day 3 pi (Fig 2C and D). These data demonstrate that the mutant virus displays virulence comparable to S300 in the absence of type I IFN signaling. When combined with our previous *in vitro* and *in vivo* studies (Cruz et al., 2010), this observation suggests that interactions with the type I IFN system contribute to the attenuation of the nsP1 T538I mutant *in vivo*, and contribute to overall protection from S300 and nsP1 T538I induced disease.

MyD88-dependent TLR signaling is dispensable for protection and control of nsP1 T538I

Given that the nsP1 T538I mutant exhibited similar levels of virulence as S300 in IFN-α/βR$^{-/-}$ mice, we sought to determine which type I IFN induction pathway(s) was responsible for regulating the attenuation of the nsP1 T538I mutant. Therefore, we assessed the role of the TLR and RLR mediated type I IFN induction pathways in the virulence of S300 and nsP1 T538I.

To begin to assess the role of the TLRs in mediating type I IFN induction, we took advantage of the fact that there are a limited number of adaptor molecules that regulate signaling by TLRs: Myd88 and TRIF (Akira, 2003). To first assess the role of the MyD88 dependent TLRs, we infected C57BL/6J and MyD88$^{-/-}$ mice i. c. with 10^3 PFU of S300 or nsP1 T538I. As shown in Fig. 3A and B, the attenuation of nsP1 T538I as compared to S300 in MyD88$^{-/-}$ mice was comparable to C57BL/6J mice, as measured by survival, MST, and weight loss, indicating that the MyD88 dependent TLRs do not contribute to the attenuation of the nsP1 T538I virus *in vivo* (Table 1–3). Furthermore, MyD88 signaling was not required for the control of replication of the nsP1 T538I virus in the brain (Fig. 3C) or spinal cord (Fig. 3D) at day 5 pi, the time-point at which control of nsP1 T538I is first observed in C57BL/6J mice. In addition, the attenuated nsP1 T538I virus phenotype was maintained in TLR7$^{-/-}$ mice (unpublished results), thus confirming the MyD88 result, and ruling out a specific role for TLR7. Taken together, these data indicate that MyD88-dependent TLR signaling does not contribute to the attenuation of the nsP1 T538I virus.

TRIF-dependent TLR signaling is not required for nsP1 T538I replication control, but does contribute to protection from virus induced disease during SINV infection

In order to evaluate the role of TRIF-dependent signaling in the pathogenesis of S300 or the nsP1 T538I mutant, we infected C57BL/6J or TRIF$^{-/-}$ mice with S300 or nsP1 T538I and measured survival and weight loss, as well as virus-induced pathology and viral burden within the brain and spinal cord. In contrast to our findings with MyD88, TRIF$^{-/-}$ mice exhibited a moderate increase in susceptibility to both S300 and nsP1 T538I viruses compared to C57BL/6J mice (Fig. 4A, B, G). TRIF$^{-/-}$ mice infected with S300 succumbed to disease with a slightly more rapid MST of 5.3 dpi, as compared to 6.7 dpi for S300 infected C57BL/6J mice, while MSTs for the nsP1 T538I virus were reduced from 9.9 days in C57BL/6J mice to 8.6 days in TRIF$^{-/-}$ mice (Table 1, 2). There was a trend towards increased mortality for TRIF$^{-/-}$ mice compared to C57BL/6J, and this difference was statistically significant for the S300 virus (Fig. 4A and Table I). For the nsP1 T538I virus, the differences in survival between wild type and TRIF$^{-/-}$ mice did not reach statistical significance (Table 1), however the pattern of increased mortality in TRIF$^{-/-}$ mice was repeatable in 3 independent experiments, suggesting that TRIF may also play a role in protecting from nsP1 T538I induced mortality. Analysis of weight loss following infection found that TRIF$^{-/-}$ mice infected with nsP1 T538I showed significantly enhanced weight loss as compared to C57BL/6J mice on 3–6 dpi (Fig. 4B, Table 3). These results further suggest that TRIF does contribute to protection against virus induced disease following both S300 and nsP1 T538I infection, though this effect was relatively modest. Furthermore, since the nsP1 T538I mutant did not show full restoration of virulence in TRIF$^{-/-}$ mice, these results suggest that other IFN induction pathways also contribute to the attenuated phenotype of the nsP1 T538I mutant.

To further assess the role of TRIF in the pathogenesis of the nsP1 T538I virus, we evaluated viral loads within the CNS at day 5 pi. Importantly, TRIF$^{-/-}$ animals showed similar levels of viral replication compared to C57BL/6J animals when infected with either S300 or nsP1 T538I. By 5 dpi, nsP1 T538I viral titers in the brains of TRIF$^{-/-}$ mice were significantly lower compared to S300 titers (Fig. 4C), and were reduced (although not statistically significant) in spinal cords (Fig. 4D). These results, which suggest that TRIF is not involved in the control of nsp1 T538I replication, were further supported by *in situ* hybridization for viral RNA within the CNS, where TRIF$^{-/-}$ mice were indistinguishable from C57BL/6J mice in terms of the distribution and intensity of viral RNA signal within the hippocampus (Fig. 4E)or brain stem (Fig. 4F) following infection with either S300 or the nsP1 T538I virus.

Given that TRIF contributes to protection from virus induced disease, but does not affect either viral loads or viral distribution within the CNS, we assessed whether TRIF deficiency might lead to enhanced pathology within the CNS of mice infected with either the S300 or nsP1 T538I viruses. As shown in Fig. 4G, S300 infection resulted in neuronal dropout within the hippocampus of C57BL/6J mice, and this was unchanged in TRIF$^{-/-}$ animals. Notably, although the nsP1 T538I virus caused reduced damage within the hippocampus of C57BL/6J mice, we report enhanced neuronal dropout in TRIF$^{-/-}$ mice. While the destruction of hippocampal neurons on their own is not likely to contribute to virus-induced mortality (Nargi-Aizenman et al., 2004), these results suggest the TRIF-dependent signaling does play a neuro-protective role independently of viral replication during infection with the nsP1 T538I virus.

IPS-1 is required for control of CNS replication and protection upon nsP1 T538I infection

Since TRIF-dependent signaling could not fully explain the attenuated phenotype of the nsP1 T538I virus, we next evaluated whether the cytoplasmic RLR pathway, which is

dependent upon the adaptor molecule IPS-1, was required to control the nsP1 T538I virus within the CNS. In contrast to the MyD88$^{-/-}$ and TRIF$^{-/-}$ mice, the nsP1 T538I virus exhibited nearly complete restoration of virulence in the IPS-1$^{-/-}$ animals, with both the wild-type S300 and nsP1 T538I viruses having nearly identical survival curves (Fig. 5A, Table 1, 2). Survival curve analysis indicates two important points: (1) the survival curve of S300 is not significantly different from that of nsP1 T538I in IPS-1$^{-/-}$ mice, and (2) both viruses cause more rapid death in IPS-1$^{-/-}$ mice compared to C57BL/6J mice. The MST of C57BL/J mice infected with S300 or nsP1 T538I were 6.1 and 10.3 dpi, respectively. However, IPS-1$^{-/-}$ mice show similar MSTs when infected with S300 or nsP1 T538I (5. 1 and 5. 4 dpi, respectively), suggesting that IPS-1 dependent signaling is required for protection from nsP1 T538I and likely S300 virus infection (Table 1, 2). We next assessed the role of IPS-1 in modulating weight loss of S300 and nsP1 T538I infected mice by statistically evaluating infected IPS-1$^{-/-}$ and C57BL/6J mice from days 0–5 pi (Fig 5B, Table 3). While there were no differences in weight loss from 0–3 dpi, on day 4 pi S300 and nsP1 T538I infected IPS-1$^{-/-}$ mice exhibited significantly different percentages of weight loss. This was also true for day 5 pi, though with the caveat being that day 5 pi data is censored due to death.

To determine the role of IPS-1 in regulating viral replication in the CNS, viral burden was assayed in the brain and spinal cords on 1, 3, and 5 dpi. There were no differences between host genotypes or virus genotypes at 1 dpi. At 3 dpi, both viruses replicated to significantly higher levels in the brains and spinal cords of IPS-1$^{-/-}$ mice as compared to C57BL/6J animals (Fig. 5C and D). On day 5 pi, the nsP1 T538I virus replicated to significantly higher levels within the brain and spinal cords of IPS-1$^{-/-}$ mice compared to C57BL/6J animals, suggesting that IPS-dependent signaling is at least partially responsible for the faster clearance of the nsP1 T538I mutant. However, nsP1 T538I titers were not fully restored to the levels of S300 in IPS-1$^{-/-}$ mice, indicating that other IFN signaling pathways also contribute to nsP1 T538I viral control. These results were confirmed by virus-specific real-time PCR, where levels of nsP1 T538I viral genomic and 26S RNA within the brains and spinal cords were significantly increased in IPS-1$^{-/-}$ mice compared to C57BL/6J mice (Fig. 6A and B). Furthermore, the nsP1 T538I virus exhibited stronger intensity and more broadly distributed viral signal within the CNS of IPS-1$^{-/-}$ mice compared to C57BL/6J animals, further suggesting that IPS-1 plays a major role in limiting nsP1 T538I replication at late times pi. However, the fact that the mutant virus did not achieve the same level of replication as S300 in IPS-1$^{-/-}$ animals suggests that other IFN induction pathways may act in concert with IPS-1 to control the nsP1 T538I mutant.

To further assess the impact of IPS-1 deficiency on protection from nsP1 T538I induced disease, we compared damage and inflammation in C57BL/6J mice and IPS-1$^{-/-}$ mice following S300 or nsP1 T538I infection. In C57BL/6J mice, S300 caused more severe neuronal damage within the hippocampus at 5 dpi than the nsP1 T538I virus. However, in IPS-1$^{-/-}$ mice, both viruses caused severe damage to neurons in the hippocampus (Fig. 6E) and cortex (unpublished results), with pyknotic neurons and significant neuronal dropout with both viruses (Fig. 6E).

Discussion

The type I IFN system plays an essential role in the control and tropism of numerous viruses, including alphaviruses (Couderc et al., 2008, Fragkoudis et al., 2007, Ryman et al., 2000, Ryman et al., 2007, Ryman and Klimstra, 2008, White et al., 2001, White et al., 2001). As a result, alphaviruses have evolved mechanisms to avoid or actively suppress the type I IFN system. Therefore, dynamic interplay between virus and host likely has major impacts on the outcome of disease. Previous work from a number of groups has

demonstrated that alphaviruses, including SINV, avoid IFN-α/β induction at least in part through their ability to nonspecifically shutoff host RNA and protein synthesis (Aguilar et al., 2007, Frolov, 2004, Frolova et al., 2002, Toribio and Ventoso, 2010). Recent studies with several different alphaviruses, including Semliki Forest virus, CHIKV, Venezuelan equine encephalitis virus, and SINV, indicate that these viruses are also able to modulate IFN-α/β induction and signaling independently of host cell shutoff (Breakwell et al., 2007, Cruz et al., 2010, Fros et al., 2010, Simmons et al., 2009, Simmons et al., 2010). In the context of SINV infection, our research group has demonstrated that a determinant at nsP1 position 538 of the neurovirulent AR86 strain of SINV modulates both IFN-α/β induction (Cruz et al., 2010) and IFN-α/β signaling in a Jak/STAT dependent manner but a host shutoff independent manner (Simmons et al., 2010). Specifically, nsP1 T538I induces greater amounts of type I IFN than S300 in both cell culture and in the serum of infected mice (Cruz et al., 2010). This determinant at nsP1 538 also plays a major role in neurovirulence, where the presence of the nsP1 538 Ile is also severely attenuating for S300 neurovirulence (Heise et al., 2000, Heise et al., 2003, Suthar et al., 2005). Therefore, we set out to determine whether the type I IFN system was required for the attenuated phenotype of the nsP1 T538I mutant *in vivo*, and if so, which host sensing pathway or pathways contributed to this phenotype. These studies clearly demonstrate that in the absence of a functional type I IFN system, the attenuated mutant is as virulent as wild type S300, and that both viruses cause more severe disease. In addition, the IPS-1-dependent host sensing pathway, and to a lesser extent, the TRIF-dependent signaling pathways contribute to this phenotype.

To our knowledge, this is the first time that IPS-1 dependent signaling has been linked to the control of a neurovirulent alphavirus. Despite the critical role of IPS-1, it does not explain all of the protection and replication control provided by type-I interferon, because IFN-α/βR$^{-/-}$ mice succumbed to infection approximately 2 days before IPS 1$^{-/-}$ mice, and IFN-α/βR$^{-/-}$ supported approximately 1.5 logs greater replication in the CNS, than did IPS-1$^{-/-}$ mice at 3 dpi. Our results are consistent with those of several other groups that have demonstrated that the cytoplasmic RNA sensing pathways play a major role in the response to alphaviruses. IPS-1 dependent signaling pathways have been shown to play a major role in IFN-α/β induction by SINV (Burke et al., 2009) and CHIKV (White et al., 2010, Schilte et al., 2010). *In vivo* studies demonstrated that IPS-1$^{-/-}$ mice support increased CHIKV replication in the serum at 48 hpi, but not in other organs or at other time-points tested (Schilte et al., 2010). While no IPS-1$^{-/-}$ mice died from infection with CHIKV, 100% of IFN-α/βR$^{-/-}$ mice infected with CHIKV died within 4 dpi (Schilte et al., 2010).

A recent study investigated the role of TLRs during infection with an independently derived neurovirulent strain of SINV, neuro-adapted SINV (NSV). Specifically, Esen et al. infected mice with a point mutation in an endoplasmic reticulum gene, *Unc93b13*$^{d/3d}$, that are incapable of signaling through TLR3, TLR7, and TLR9. These mice fail to transfer TLRs from the ER to the endosome (Esen et al., 2012, Kim et al., 2008, Tabeta et al., 2006). While *Unc93b13*$^{d/3d}$ mice were more susceptible to SINV strain NSV infection, neither MyD88$^{-/-}$ nor TLR3$^{-/-}$ mice were more susceptible, suggesting that TLRs do not regulate the pathogenesis to NSV infection (Esen et al., 2012). Consistent with these results, we did not find a role for MyD88 in protecting mice during infection with either the wild type S300 or the mutant nsP1 T538I virus. However, in contrast to the results with NSV, we did find that TRIF dependent signaling plays a modest role in protecting from virus induced disease and neuronal damage following infection with both the wild type and mutant AR86 viruses. Though it remains to be determined why TRIF dependent signaling plays a different role during AR86 and NSV infection, these results do indicate that these two neurovirulent virus strains do differ somewhat in their interactions with the host.

Based on the critical protective role for IPS-1 in nsP1 T538I pathogenesis, we are currently assessing the roles of RIG-I and Mda5 in sensing the nsP1 T538I mutant. We have previously shown that the nsP1 T538I mutation leads to enhanced 26S RNA synthesis. Since RIG-I and Mda5 recognize viral RNA, the nsP1 T538I virus may be producing more ligand in virally infected cells compared to wild-type S300 (Heise et al., 2003). Studies are currently underway to evaluate whether enhanced 26S RNA expression or some other aspect of the nsP1 T538I mutant virus life cycle leads to enhanced type I IFN induction via IPS-1, TRIF, or interactions between the two pathways compared to wild-type S300. Furthermore, we have demonstrated that TLR4 is not required for protection from nsP1 T538I disease (unpublished results), suggesting that TLR3-dependent signaling may be responsible for the protective role of TRIF, and therefore TLR3$^{-/-}$ mice are currently being tested.

Another possible explanation for why IPS-1$^{-/-}$ mice are not as susceptible to SINV as IFNα/βR$^{-/-}$ mice is that IFN signaling is critical for protection. Even a small amount of type I IFN can be amplified through IFN signaling on infected and uninfected cells. IFN signaling is functional in IPS-1$^{-/-}$ mice, and we have found that type I IFN is still produced in IPS-1$^{-/-}$ mice (unpublished results). Although IFNα/βR$^{-/-}$ produce type I IFN, they are incapable of responding, possibly explaining the extreme susceptibility.

Type I IFNs exert antiviral effects through the upregulation of ISGs, which possess antiviral activity, and by stimulating the adaptive immune response (Coro et al., 2006, Fink et al., 2006, Havenar-Daughton et al., 2006, Purtha et al., 2008). Several ISGs, such as Viperin, ZAP, ISG15, ISG12, ISG20, and PKR have been shown to contribute to control of alphavirus (Bick et al., 2003, Giannakopoulos et al., 2009, Labrada et al., 2002, Lenschow et al., 2005, Lenschow et al., 2007, MacDonald et al., 2007, Ryman et al., 2005, Zhang et al., 2007), and future studies will address whether IPS-1-dependent expression of these or other ISGs have antiviral activity against the nsP1 T538I virus.

Adaptive immune pathways, namely antibody, IFN-γ, and T cells, also play key roles in SINV control and clearance (Binder and Griffin, 2001, Burdeinick-Kerr and Griffin, 2005, Burdeinick-Kerr et al., 2009, Byrnes et al., 2000, Griffin et al., 1997, Griffin, 2010). IPS-1 has previously been shown to modulate the adaptive immune response during West Nile virus infection (Suthar et al., 2010), and thus it will also be important to determine if RLR signaling contributes to virus-specific T cell or antibody responses via IPS-1. We have seen no difference in the quantity of serum anti-SINV antibodies or neutralizing antibody production between S300 and nsP1 T538I infected C57BL/6J at 6 dpi (unpublished results). Evidence has shown that IPS-1 and TRIF cooperatively contribute to the adjuvant effects of poly:IC, a result that was only determined by examining the IPS-1 and TRIF double knockout mouse (Kumar et al., 2008). While we have shown the independent roles of the TLR and RLR pathways, studies are underway to test how these pathways might cooperatively interact.

Conclusions

In summary, we have demonstrated that the type I IFN pathway via IPS-1, but not TLR-dependent signaling pathways are essential for controlling nsP1 T538I replication. Furthermore, IPS-1, and to a lesser extent TRIF-dependent signaling protected mice from nsP1 T538I and S300 induced disease. These studies suggest that the *in vivo* attenuation of the nsP1 T538I virus is predominantly regulated by the IPS-1-dependent sensing pathway.

Materials and Methods

Mice

Female C57BL/6J, TRIF/Ticam-1 deficient (stock 005037), and MyD88 deficient (stock 009088) mice were obtained commercially from Jackson Labs. IFN-α/βR$^{-/-}$ mice on the C57BL/6J background were provided by Jason Whitmire (UNC-Chapel Hill), and were originally made by Jonathan Sprent (The Scripps Research Institute) (Kolumam et al., 2005). IPS-1$^{-/-}$ (STI) mice were generated in the Gale laboratory as previously described (65). Mice were genotyped and bred in house under specific-pathogen-free conditions. Adult 9–12–week–old female mice were anesthetized with a ketamine-xylazine mixture prior to intracranial (i.c.) inoculation with 10^3 PFU of virus in diluent (Dulbecco's Phosphate Buffered Saline [1X DPBS; GIBCO] supplemented with 1% donor calf serum (DCS), 0. 122 mg/mL $CaCl_2$, and 0. 10 mg/mL MgCl); total volume, 10μl). Mock infected mice received diluents alone. Mice were weighed daily and monitored for disease signs. As required by the UNC CH Institutional Animal Care and Use Committee (IACUC), infected mice were euthanized during the experiment either when mice dropped below 70% of initial body weight or when mice exhibited severe disease signs. Mouse experiments were approved and performed in accordance with all IACUC guidelines.

Viral burden analysis

For *in vivo* growth studies, mice were inoculated as above and sacrificed by exsanguination followed by perfusion with 15 ml of PBS. Indicated tissues were removed, weighed, homogenized using glass-beads in a tissue homogenizer and stored at −80°C until viral load was assessed by a standard plaque assay on baby hamster kidney (BHK-21) cells as previously described (Heise et al., 2000).

Virus production

The wild-type AR86 infectious clone is denoted as S300, and the mutant virus with a single amino acid change (nsP1 T538I) is denoted as S340. Both pS300 and pS55 plasmids, which differ only in the linearization site used, each encode wild type AR86; thus, S300 and the previously designated S55 (Heise et al., 2000, Heise et al., 2003) are synonymous. Similarly, S51 is synonymous with S340/nsP1 T538I (Heise et al., 2000, Suthar et al., 2005). Virus stocks were made as described previously (Heise et al., 2000). Briefly, viral cDNA plasmids were linearized with PmeI and used as templates for the synthesis of full-length transcripts by using SP6-specific mMessage Machine *in vitro* transcription kits (Ambion). Capped, poly-adenylated transcripts were then electroporated into BHK-21 cells, and after 24 hours, supernatants were harvested, and clarified at 3,000 RPM for 15 minutes. All virus stocks were titrated by plaque assay on BHK-21 cells.

In situ hybridization

Hybridizations were performed with a ^{35}S-UTP-labeled AR86-specifec riboprobe derived from pDS-45. Clone pDS-45 was constructed, linearized, and transcribed as described previously (Heise et al., 2000). This riboprobe encodes the last 187 nucleotides of the nsP4 gene, the 26S promoter region, and the first 209 nucleotides of the capsid gene. A riboprobe specific for Epstein-Barr virus was used as a control probe for nonspecific binding. The AR86 probe was hybridized to tissues from PBS-inoculated mice as an additional control for nonspecific binding. The *in situ* hybridizations were performed according to the method of Charles *et al.,* (Charles et al., 1995) by using 25 μL of probe/slide at 5×10^4 cpm/μL.

Histological analysis

Mock-infected or SINV-infected mice were sacrificed by exsanguination followed by perfusion with 15 ml of PBS, 4% paraformaldehyde (PFA), pH 7.3. Brains were embedded in paraffin and 10μm sections were prepared and stained with hematoxylin and eosin (H&E) by the UNC histopathology core facility. Sections were analyzed using an Olympus BX61 microscope fitted with a QImaging RETIGA 4000R color camera for digital imaging.

Real-time PCR

For SINV genome analysis, a TaqMan primer-probe set (designed with the Primer Express software) specific for the nsP3 and the E2 region of SINV were used. The primer and probe sequences for the TaqMan primer-probe set were as follows: nsP3: forward primer, 5 – ATATCGCCTCGTTCGACAAAA-3 ; reverse primer, 5 – ACACCCAGGTCTTCCAAGATCA-3 ; and probe, 5 – TATGGCGTTAACCGGCCT-3 , E2: forward primer, 5 –CGCGGCCTGGTGTACAAC-3 ; reverse primer, 5 – CCAAACGCTCCTGGTTTCA-3 ; and probe, 5 – TGACTTTCCGGAATACGGA-3 . Brain RNA was isolated with an RNeasy Lipid Tissue Mini kit (Qiagen). cDNAs were synthesized from mRNA by reverse transcription with the respective tagged primer. RT PCR (qRT-PCR) was then performed with Prism 7000 real-time PCR system. cDNA standard curves for the SINV genome and 26S RNA were generated to ensure optimal primer-probe efficiency and to assign relative genome and 26S RNA copy numbers to directly compare each sample.

Statistical Analysis

Differences in Kaplan-Meier survival curves were analyzed by Mantel-Haenszel test. Weight loss curves across days were initially analyzed by MANOVA. If overall differences were observed across weight loss curves, ANOVA and Tukey's Honestly Significant Difference test were used to determine factors influencing weight-loss within a given day. Survival curves and weight loss data were analyzed using the R statistical language (R Development Core Team, 2010), with the survival package for survival analysis. For *in vivo* viral burden analysis, a two-way ANOVA, with Bonferonni correction was used to determine statistical differences. Viral burden data were analyzed using Prism software (GraphPad Prism5, San Diego, CA).

Acknowledgments

References

Aguilar PV, Weaver SC, Basler CF. Capsid protein of eastern equine encephalitis virus inhibits host cell gene expression. J.Virol. 2007; 81:3866–3876. [PubMed: 17267491]

Akira S. Mammalian Toll-like receptors. Curr.Opin.Immunol. 2003; 15:5–11. [PubMed: 12495726]

Bick MJ, Carroll JW, Gao G, Goff SP, Rice CM, MacDonald MR. Expression of the zinc-finger antiviral protein inhibits alphavirus replication. J.Virol. 2003; 77:11555–11562. [PubMed: 14557641]

Binder GK, Griffin DE. Interferon-gamma-mediated site-specific clearance of alphavirus from CNS neurons. Science. 2001; 293:303–306. [PubMed: 11452126]

Breakwell L, Dosenovic P, Karlsson Hedestam GB, D'Amato M, Liljestrom P, Fazakerley J, McInerney GM. Semliki Forest virus nonstructural protein 2 is involved in suppression of the type I interferon response. J.Virol. 2007; 81:8677–8684. [PubMed: 17553895]

Brennan K, Bowie AG. Activation of host pattern recognition receptors by viruses. Curr.Opin.Microbiol. 2010; 13:503–507. [PubMed: 20538506]

Burdeinick-Kerr R, Govindarajan D, Griffin DE. Noncytolytic clearance of sindbis virus infection from neurons by gamma interferon is dependent on Jak/STAT signaling. J.Virol. 2009; 83:3429–3435. [PubMed: 19176616]

Burdeinick-Kerr R, Griffin DE. Gamma interferon-dependent, noncytolytic clearance of sindbis virus infection from neurons in vitro. J.Virol. 2005; 79:5374–5385. [PubMed: 15827152]

Burke CW, Gardner CL, Steffan JJ, Ryman KD, Klimstra WB. Characteristics of alpha/beta interferon induction after infection of murine fibroblasts with wild-type and mutant alphaviruses. Virology. 2009; 395:121–132. [PubMed: 19782381]

Byrnes AP, Durbin JE, Griffin DE. Control of Sindbis virus infection by antibody in interferon-deficient mice. J.Virol. 2000; 74:3905–3908. [PubMed: 10729167]

Charles PC, Walters E, Margolis F, Johnston RE. Mechanism of neuroinvasion of Venezuelan equine encephalitis virus in the mouse. Virology. 1995; 208:662–671. [PubMed: 7747437]

Colonna M. TLR pathways and IFN-regulatory factors: to each its own. Eur.J.Immunol. 2007; 37:306–309. [PubMed: 17273997]

Coro ES, Chang WL, Baumgarth N. Type I IFN receptor signals directly stimulate local B cells early following influenza virus infection. J.Immunol. 2006; 176:4343–4351. [PubMed: 16547272]

Couderc T, Chretien F, Schilte C, Disson O, Brigitte M, Guivel-Benhassine F, Touret Y, Barau G, Cayet N, Schuffenecker I, Despres P, Arenzana-Seisdedos F, Michault A, Albert ML, Lecuit M. A mouse model for Chikungunya: young age and inefficient type-I interferon signaling are risk factors for severe disease. PLoS Pathog. 2008; 4:e29. [PubMed: 18282093]

Cruz CC, Suthar MS, Montgomery SA, Shabman R, Simmons J, Johnston RE, Morrison TE, Heise MT. Modulation of type I IFN induction by a virulence determinant within the alphavirus nsP1 protein. Virology. 2010; 399:1–10. [PubMed: 20097400]

Diebold SS, Kaisho T, Hemmi H, Akira S, Reis e Sousa C. Innate antiviral responses by means of TLR7-mediated recognition of single-stranded RNA. Science. 2004; 303:1529–1531. [PubMed: 14976261]

Dropulic LK, Hardwick JM, Griffin DE. A single amino acid change in the E2 glycoprotein of Sindbis virus confers neurovirulence by altering an early step of virus replication. J.Virol. 1997; 71:6100–6105. [PubMed: 9223504]

Esen N, Blakely PK, Rainey-Barger EK, Irani DN. Complexity of the microglial activation pathways that drive innate host responses during lethal alphavirus encephalitis in mice. ASN Neuro. 2012

Fink K, Lang KS, Manjarrez-Orduno N, Junt T, Senn BM, Holdener M, Akira S, Zinkernagel RM, Hengartner H. Early type I interferon-mediated signals on B cells specifically enhance antiviral humoral responses. Eur.J.Immunol. 2006; 36:2094–2105. [PubMed: 16810635]

Fragkoudis R, Breakwell L, McKimmie C, Boyd A, Barry G, Kohl A, Merits A, Fazakerley JK. The type I interferon system protects mice from Semliki Forest virus by preventing widespread virus dissemination in extraneural tissues, but does not mediate the restricted replication of avirulent virus in central nervous system neurons. J.Gen.Virol. 2007; 88:3373–3384. [PubMed: 18024907]

Frolov I. Persistent infection and suppression of host response by alphaviruses. Arch.Virol.Suppl. 2004; 18:139–147. [PubMed: 15119769]

Frolova EI, Fayzulin RZ, Cook SH, Griffin DE, Rice CM, Frolov I. Roles of nonstructural protein nsP2 and Alpha/Beta interferons in determining the outcome of Sindbis virus infection. J.Virol. 2002; 76:11254–11264. [PubMed: 12388685]

Fros JJ, Liu WJ, Prow NA, Geertsema C, Ligtenberg M, Vanlandingham DL, Schnettler E, Vlak JM, Suhrbier A, Khromykh AA, Pijlman GP. Chikungunya virus nonstructural protein 2 inhibits type I/II interferon-stimulated JAK-STAT signaling. J.Virol. 2010; 84:10877–10887. [PubMed: 20686047]

Giannakopoulos NV, Arutyunova E, Lai C, Lenschow DJ, Haas AL, Virgin HW. ISG15 Arg151 and the ISG15-conjugating enzyme UbE1L are important for innate immune control of Sindbis virus. J.Virol. 2009; 83:1602–1610. [PubMed: 19073728]

Gitlin L, Barchet W, Gilfillan S, Cella M, Beutler B, Flavell RA, Diamond MS, Colonna M. Essential role of mda-5 in type I IFN responses to polyriboinosinic:polyribocytidylic acid and encephalomyocarditis picornavirus. Proc.Natl.Acad.Sci.U.S.A. 2006; 103:8459–8464. [PubMed: 16714379]

Griffin D, Levine B, Tyor W, Ubol S, Despres P. The role of antibody in recovery from alphavirus encephalitis. Immunol.Rev. 1997; 159:155–161. [PubMed: 9416509]

Griffin DE. Recovery from viral encephalomyelitis: immune-mediated noncytolytic virus clearance from neurons. Immunol.Res. 2010; 47:123–133. [PubMed: 20087684]

Griffin DE, Levine B, Tyor WR, Tucker PC, Hardwick JM. Age-dependent susceptibility to fatal encephalitis: alphavirus infection of neurons. Arch.Virol.Suppl. 1994; 9:31–39. [PubMed: 8032263]

Havenar-Daughton C, Kolumam GA, Murali-Krishna K. Cutting Edge: The direct action of type I IFN on CD4 T cells is critical for sustaining clonal expansion in response to a viral but not a bacterial infection. J.Immunol. 2006; 176:3315–3319. [PubMed: 16517698]

Heise MT, Simpson DA, Johnston RE. A single amino acid change in nsP1 attenuates neurovirulence of the Sindbis-group alphavirus S.A.AR86. J.Virol. 2000; 74:4207–4213. [PubMed: 10756033]

Heise MT, White LJ, Simpson DA, Leonard C, Bernard KA, Meeker RB, Johnston RE. An attenuating mutation in nsP1 of the Sindbis-group virus S.A.AR86 accelerates nonstructural protein processing and up-regulates viral 26S RNA synthesis. J.Virol. 2003; 77:1149–1156. [PubMed: 12502831]

Hiscott J. Triggering the innate antiviral response through IRF-3 activation. J.Biol.Chem. 2007; 282:15325–15329. [PubMed: 17395583]

Horner SM, Liu HM, Park HS, Briley J, Gale M Jr. Mitochondrial-associated endoplasmic reticulum membranes (MAM) form innate immune synapses and are targeted by hepatitis C virus. Proc.Natl.Acad.Sci.U.S.A. 2011; 108:14590–14595. [PubMed: 21844353]

Hornung V, Ellegast J, Kim S, Brzozka K, Jung A, Kato H, Poeck H, Akira S, Conzelmann KK, Schlee M, Endres S, Hartmann G. 5'-Triphosphate RNA is the ligand for RIG-I. Science. 2006; 314:994–997. [PubMed: 17038590]

Janeway CA Jr. Approaching the asymptote? Evolution and revolution in immunology. Cold Spring Harb.Symp.Quant.Biol. 1989; 54(Pt 1):1–13. [PubMed: 2700931]

Johnson RT, McFarland HF, Levy SE. Age-dependent resistance to viral encephalitis: studies of infections due to Sindbis virus in mice. J.Infect.Dis. 1972; 125:257–262. [PubMed: 4552644]

Kato H, Takeuchi O, Mikamo-Satoh E, Hirai R, Kawai T, Matsushita K, Hiiragi A, Dermody TS, Fujita T, Akira S. Length-dependent recognition of double-stranded ribonucleic acids by retinoic acid-inducible gene-I and melanoma differentiation-associated gene 5. J.Exp.Med. 2008; 205:1601–1610. [PubMed: 18591409]

Kato H, Takeuchi O, Sato S, Yoneyama M, Yamamoto M, Matsui K, Uematsu S, Jung A, Kawai T, Ishii KJ, Yamaguchi O, Otsu K, Tsujimura T, Koh CS, Reis e Sousa C, Matsuura Y, Fujita T, Akira S. Differential roles of MDA5 and RIG-I helicases in the recognition of RNA viruses. Nature. 2006; 441:101–105. [PubMed: 16625202]

Kawai T, Akira S. Toll-like receptors and their crosstalk with other innate receptors in infection and immunity. Immunity. 2011; 34:637–650. [PubMed: 21616434]

Kawai T, Akira S. Antiviral signaling through pattern recognition receptors. J.Biochem. 2007; 141:137–145. [PubMed: 17190786]

Kim YM, Brinkmann MM, Paquet ME, Ploegh HL. UNC93B1 delivers nucleotidesensing toll-like receptors to endolysosomes. Nature. 2008; 452:234–238. [PubMed: 18305481]

Kobiler D, Rice CM, Brodie C, Shahar A, Dubuisson J, Halevy M, Lustig S. A single nucleotide change in the 5' noncoding region of Sindbis virus confers neurovirulence in rats. J.Virol. 1999; 73:10440–10446. [PubMed: 10559362]

Kolumam GA, Thomas S, Thompson LJ, Sprent J, Murali-Krishna K. Type I interferons act directly on CD8 T cells to allow clonal expansion and memory formation in response to viral infection. J.Exp.Med. 2005; 202:637–650. [PubMed: 16129706]

Kumar H, Kawai T, Kato H, Sato S, Takahashi K, Coban C, Yamamoto M, Uematsu S, Ishii KJ, Takeuchi O, Akira S. Essential role of IPS-1 in innate immune responses against RNA viruses. J.Exp.Med. 2006; 203:1795–1803. [PubMed: 16785313]

Kumar H, Koyama S, Ishii KJ, Kawai T, Akira S. Cutting edge: cooperation of IPS- 1- and TRIF-dependent pathways in poly IC-enhanced antibody production and cytotoxic T cell responses. J.Immunol. 2008; 180:683–687. [PubMed: 18178804]

Labrada L, Liang XH, Zheng W, Johnston C, Levine B. Age-dependent resistance to lethal alphavirus encephalitis in mice: analysis of gene expression in the central nervous system and identification of a novel interferon-inducible protective gene, mouse ISG12. J.Virol. 2002; 76:11688–11703. [PubMed: 12388728]

Lenschow DJ, Giannakopoulos NV, Gunn LJ, Johnston C, O'Guin AK, Schmidt RE, Levine B, Virgin HW 4th. Identification of interferon-stimulated gene 15 as an antiviral molecule during Sindbis virus infection in vivo. J.Virol. 2005; 79:13974–13983. [PubMed: 16254333]

Lenschow DJ, Lai C, Frias-Staheli N, Giannakopoulos NV, Lutz A, Wolff T, Osiak A, Levine B, Schmidt RE, Garcia-Sastre A, Leib DA, Pekosz A, Knobeloch KP, Horak I, Virgin HW 4th. IFN-stimulated gene 15 functions as a critical antiviral molecule against influenza, herpes, and Sindbis viruses. Proc.Natl.Acad.Sci.U.S.A. 2007; 104:1371–1376. [PubMed: 17227866]

Loo YM, Fornek J, Crochet N, Bajwa G, Perwitasari O, Martinez-Sobrido L, Akira S, Gill MA, Garcia-Sastre A, Katze MG, Gale Jr. Distinct RIG-I and MDA5 signaling by RNA viruses in innate immunity. J.Virol. 2008; 82:335–345. [PubMed: 17942531]

Lund JM, Alexopoulou L, Sato A, Karow M, Adams NC, Gale NW, Iwasaki A, Flavell RA. Recognition of single-stranded RNA viruses by Toll-like receptor 7. Proc.Natl.Acad.Sci.U.S.A. 2004; 101:5598–5603. [PubMed: 15034168]

MacDonald MR, Machlin ES, Albin OR, Levy DE. The zinc finger antiviral protein acts synergistically with an interferon-induced factor for maximal activity against alphaviruses. J.Virol. 2007; 81:13509–13518. [PubMed: 17928353]

Matsumoto M, Funami K, Oshiumi H, Seya T. Toll-like receptor 3: a link between toll-like receptor, interferon and viruses. Microbiol.Immunol. 2004; 48:147–154. [PubMed: 15031527]

Matsumoto M, Oshiumi H, Seya T. Antiviral responses induced by the TLR3 pathway. Rev.Med.Virol. 2011

Nallagatla SR, Hwang J, Toroney R, Zheng X, Cameron CE, Bevilacqua PC. 5'- triphosphate-dependent activation of PKR by RNAs with short stem-loops. Science. 2007; 318:1455–1458. [PubMed: 18048689]

Nargi-Aizenman JL, Havert MB, Zhang M, Irani DN, Rothstein JD, Griffin DE. Glutamate receptor antagonists protect from virus-induced neural degeneration. Ann.Neurol. 2004; 55:541–549. [PubMed: 15048893]

Oshiumi H, Matsumoto M, Funami K, Akazawa T, Seya T. TICAM-1, an adaptor molecule that participates in Toll-like receptor 3-mediated interferon-beta induction. Nat.Immunol. 2003; 4:161–167. [PubMed: 12539043]

Park E, Griffin DE. The nsP3 macro domain is important for Sindbis virus replication in neurons and neurovirulence in mice. Virology. 2009; 388:305–314. [PubMed: 19395054]

Pichlmair A, Schulz O, Tan CP, Naslund TI, Liljestrom P, Weber F, Reis e Sousa C. RIG-I-mediated antiviral responses to single-stranded RNA bearing 5'-phosphates. Science. 2006; 314:997–1001. [PubMed: 17038589]

Purtha WE, Chachu KA, Virgin HW 4th, Diamond MS. Early B-cell activation after West Nile virus infection requires alpha/beta interferon but not antigen receptor signaling. J.Virol. 2008; 82:10964–10974. [PubMed: 18786989]

R Development Core Team. R: A language and environment for statistical computing. 2010.

Ryman KD, Klimstra WB. Host responses to alphavirus infection. Immunol.Rev. 2008; 225:27–45. [PubMed: 18837774]

Wollish et al.

Ryman KD, Klimstra WB, Nguyen KB, Biron CA, Johnston RE. Alpha/beta interferon protects adult mice from fatal Sindbis virus infection and is an important determinant of cell and tissue tropism. J.Virol. 2000; 74:3366–3378. [PubMed: 10708454]

Ryman KD, Meier KC, Gardner CL, Adegboyega PA, Klimstra WB. Nonpathogenic Sindbis virus causes hemorrhagic fever in the absence of alpha/beta and gamma interferons. Virology. 2007; 368:273–285. [PubMed: 17681583]

Ryman KD, Meier KC, Nangle EM, Ragsdale SL, Korneeva NL, Rhoads RE, MacDonald MR, Klimstra WB. Sindbis virus translation is inhibited by a PKR/RNase L-independent effector induced by alpha/beta interferon priming of dendritic cells. J.Virol. 2005; 79:1487–1499. [PubMed: 15650175]

Sasai M, Tatematsu M, Oshiumi H, Funami K, Matsumoto M, Hatakeyama S, Seya T. Direct binding of TRAF2 and TRAF6 to TICAM-1/TRIF adaptor participates in activation of the Toll-like receptor 3/4 pathway. Mol.Immunol. 2010; 47:1283–1291. [PubMed: 20047764]

Schilte C, Couderc T, Chretien F, Sourisseau M, Gangneux N, Guivel-Benhassine F, Kraxner A, Tschopp J, Higgs S, Michault A, Arenzana-Seisdedos F, Colonna M, Peduto L, Schwartz O, Lecuit M, Albert ML. Type I IFN controls chikungunya virus via its action on nonhematopoietic cells. J.Exp.Med. 2010; 207:429–442. [PubMed: 20123960]

Simmons JD, White LJ, Morrison TE, Montgomery SA, Whitmore AC, Johnston RE, Heise MT. Venezuelan equine encephalitis virus disrupts STAT1 signaling by distinct mechanisms independent of host shutoff. J.Virol. 2009; 83:10571–10581. [PubMed: 19656875]

Simmons JD, Wollish AC, Heise MT. A Determinant of Sindbis Virus Neurovirulence Enables Efficient Disruption of Jak/STAT Signaling. J.Virol. 2010; 84:11429–11439. [PubMed: 20739538]

Simpson DA, Davis NL, Lin SC, Russell D, Johnston RE. Complete nucleotide sequence and full-length cDNA clone of S.A.AR86 a South African alphavirus related to Sindbis. Virology. 1996; 222:464–469. [PubMed: 8806532]

Suthar MS, Ma DY, Thomas S, Lund JM, Zhang N, Daffis S, Rudensky AY, Bevan MJ, Clark EA, Kaja MK, Diamond MS, Gale M Jr. IPS-1 is essential for the control of West Nile virus infection and immunity. PLoS Pathog. 2010; 6:e1000757. [PubMed: 20140199]

Suthar MS, Shabman R, Madric K, Lambeth C, Heise MT. Identification of adult mouse neurovirulence determinants of the Sindbis virus strain AR86. J.Virol. 2005; 79:4219–4228. [PubMed: 15767423]

Tabeta K, Hoebe K, Janssen EM, Du X, Georgel P, Crozat K, Mudd S, Mann N, Sovath S, Goode J, Shamel L, Herskovits AA, Portnoy DA, Cooke M, Tarantino LM, Wiltshire T, Steinberg BE, Grinstein S, Beutler B. The Unc93b1 mutation 3d disrupts exogenous antigen presentation and signaling via Toll-like receptors 3, 7 and 9. Nat.Immunol. 2006; 7:156–164. [PubMed: 16415873]

Toribio R, Ventoso I. Inhibition of host translation by virus infection in vivo. Proc.Natl.Acad.Sci.U.S.A. 2010; 107:9837–9842. [PubMed: 20457920]

Tucker PC, Lee SH, Bui N, Martinie D, Griffin DE. Amino acid changes in the Sindbis virus E2 glycoprotein that increase neurovirulence improve entry into neuroblastoma cells. J.Virol. 1997; 71:6106–6112. [PubMed: 9223505]

Tucker PC, Strauss EG, Kuhn RJ, Strauss JH, Griffin DE. Viral determinants of age-dependent virulence of Sindbis virus for mice. J.Virol. 1993; 67:4605–4610. [PubMed: 8392602]

Uematsu S, Akira S. Innate immune recognition of viral infection. Uirusu. 2006; 56:1–8. [PubMed: 17038806]

WEINBREN MP, KOKERNOT RH, SMITHBURN KC. Strains of Sindbis-like virus isolated from culicine mosquitoes in the Union of South AfricaIIsolation and properties. S.Afr.Med.J. 1956; 30:631–636. [PubMed: 13351869]

White L, Sali T, Alvarado D, Gatti E, Pierre P, Streblow D, Defilippis VR. Chikungunya Virus Induces IPS-1-Dependent Innate Immune Activation and PKR-Independent Translational Shutoff. J.Virol. 2010

White LJ, Wang JG, Davis NL, Johnston RE. Role of alpha/beta interferon in Venezuelan equine encephalitis virus pathogenesis: effect of an attenuating mutation in the 5' untranslated region. J.Virol. 2001; 75:3706–3718. [PubMed: 11264360]

Yamamoto M, Sato S, Hemmi H, Hoshino K, Kaisho T, Sanjo H, Takeuchi O, Sugiyama M, Okabe M, Takeda K, Akira S. Role of adaptor TRIF in the MyD88- independent toll-like receptor signaling pathway. Science. 2003; 301:640–643. [PubMed: 12855817]

Yin J, Gardner CL, Burke CW, Ryman KD, Klimstra WB. Similarities and differences in antagonism of neuron alpha/beta interferon responses by Venezuelan equine encephalitis and Sindbis alphaviruses. J.Virol. 2009; 83:10036–10047. [PubMed: 19641001]

Yokota S, Okabayashi T, Fujii N. The battle between virus and host: modulation of Toll-like receptor signaling pathways by virus infection. Mediators Inflamm. 2010; 2010:184328. [PubMed: 20672047]

Zhang Y, Burke CW, Ryman KD, Klimstra WB. Identification and characterization of interferon-induced proteins that inhibit alphavirus replication. J.Virol. 2007; 81:11246–11255. [PubMed: 17686841]

Highlights

IPS-1 is essential for protection and control of an attenuated Sindbis virus.

TRIF plays a modest role in protection from Sindbis-induced neurologic disease.

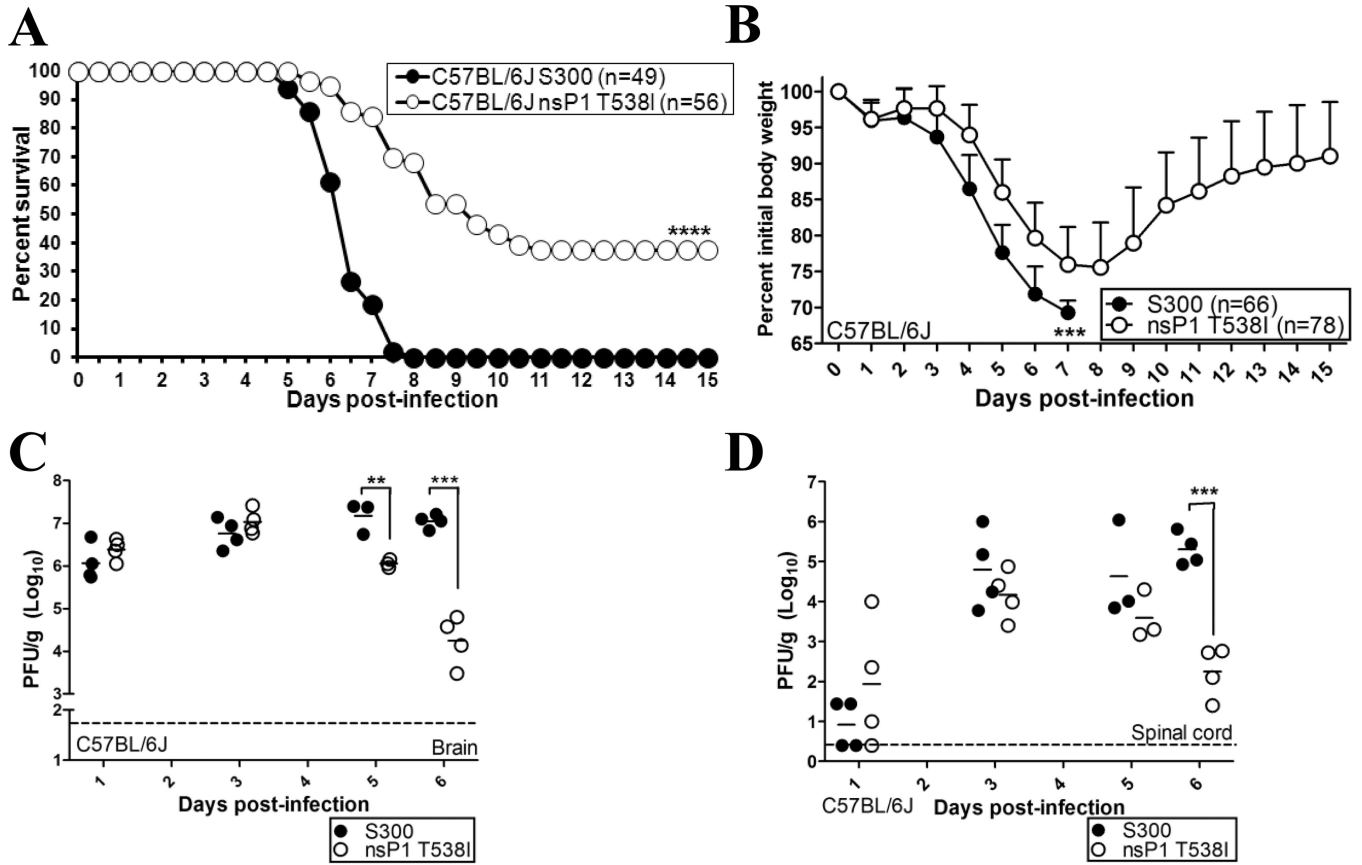MyD88 does not regulate Sindbis neurovirulence.

Figure 1. The mutant virus nsP1 T538I is attenuated in C57BL/6J mice as compared to S300 wild-type virus

Adult 9–12 week old female C57BL/6J mice were infected i.c. with 10^3 PFU of S300 or nsP1 T538I virus and monitored daily for (A) survival, (B) weight loss, and (C) brain and (D) spinal cords were harvested at 1, 3, 5, and 6 days post infection for viral titer by plaque assay. Survival data are presented as the pooled results of at least 3 experiments. Weight loss data are presented as the means + the standard deviation of 16 experiments. Viral titer data are shown as the mean of a single experiment and are representative of at least three experiments. The number of mice infected per virus is indicated in parentheses. Asterisks denote $p < 0.01$(**), $p < 0.001$(***), or $p < 0.0001$(****). The horizontal dashed line indicates the lower limit of assay sensitivity.

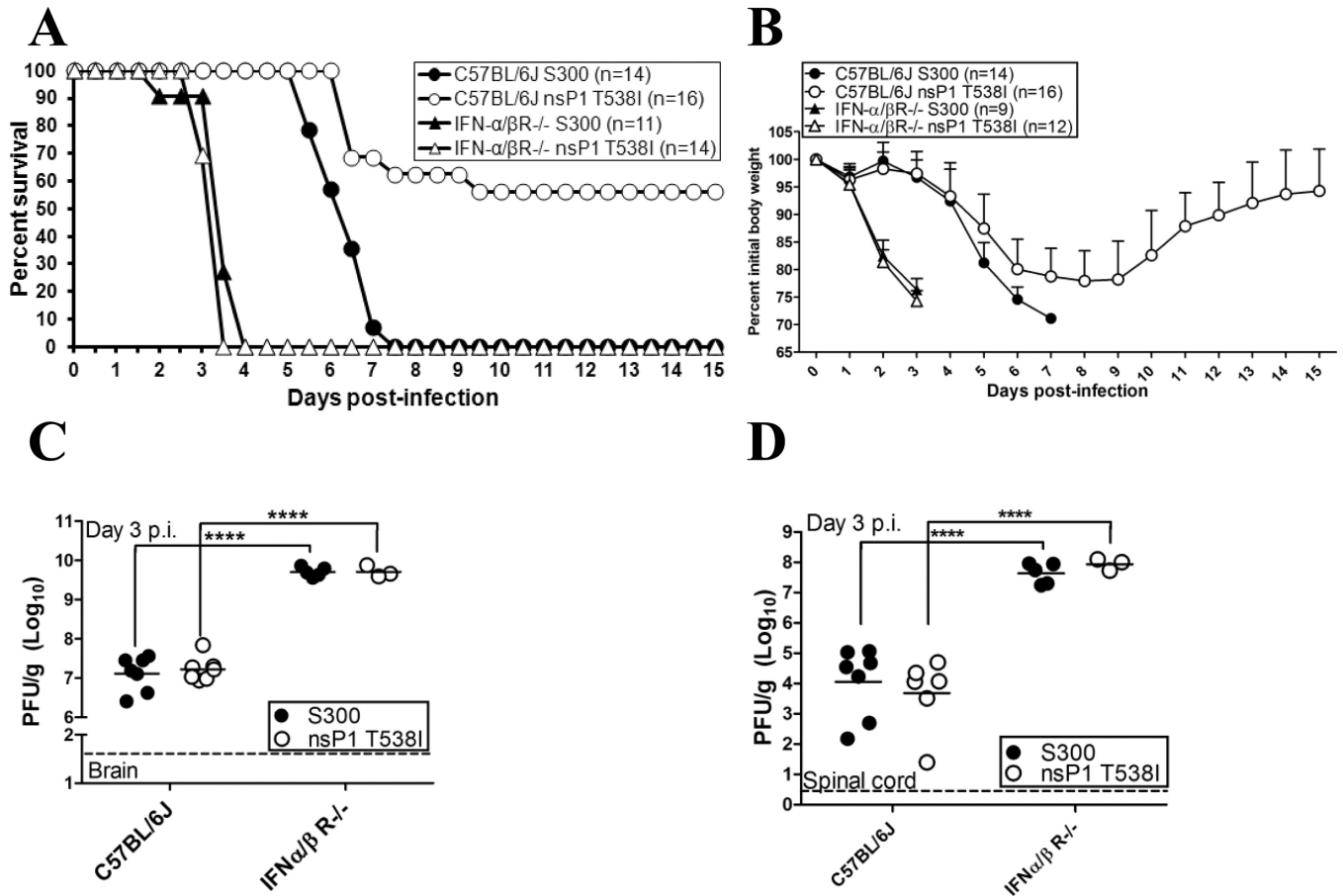**Figure 2. Both S300 and nsP1 T538I show equivalent and enhanced virulence in the absence of the IFN-α/β response**

Adult 9–12 week old female C57BL/6J and IFN-α/βR deficient mice were infected i.c. with 10^3 PFU of S300 or nsP1 T538I virus. Equivalent and rapid (A) lethality and (B) weight loss with both S300 and nsP1 T538I infection of IFN-α/βR$^{-/-}$ mice. The number of mice infected per virus is indicated in parentheses, and data are compiled from a minimum of two experiments. Infectious virus data are shown as the mean of 2 pooled experiments, and was assayed at day 3 pi within the (C) brain and (D) spinal cord of C57BL/6J and IFN-α/βR$^{-/-}$ mice. Asterisks denote $p < 0.0001$(****). The dashed line indicates the lower limit of assay sensitivity.
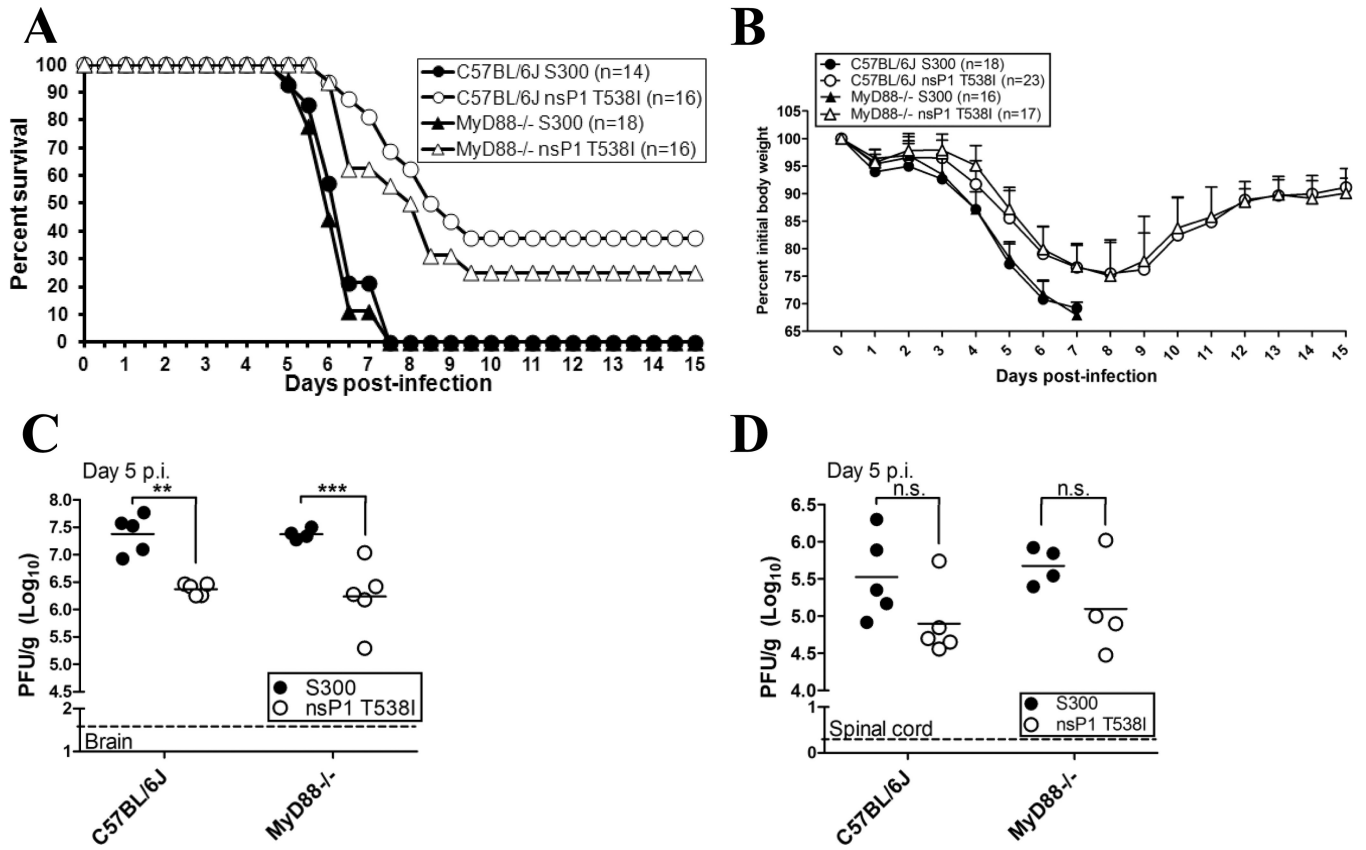
Figure 3. TLR signaling through MyD88 is not required for protection or control of nsP1 T538I infection

Adult 9–12-week-old female C57BL/6J and MyD88$^{-/-}$ mice were infected i.c. with 10^3 PFU of S300 or nsP1 T538I virus. Differential (A) survival and (B) weight loss between S300 and nsP1 T538I infected MyD88$^{-/-}$ mice. The number of mice infected per group is indicated in parentheses. Infectious virus was assayed at 5 days pi in the (C) brain and (D) spinal cord. Asterisks denote $p < 0.01$(**) or $p < 0.001$(***). Titer data are representative of two or more experiments. The dashed line indicates the lower limit of assay sensitivity.
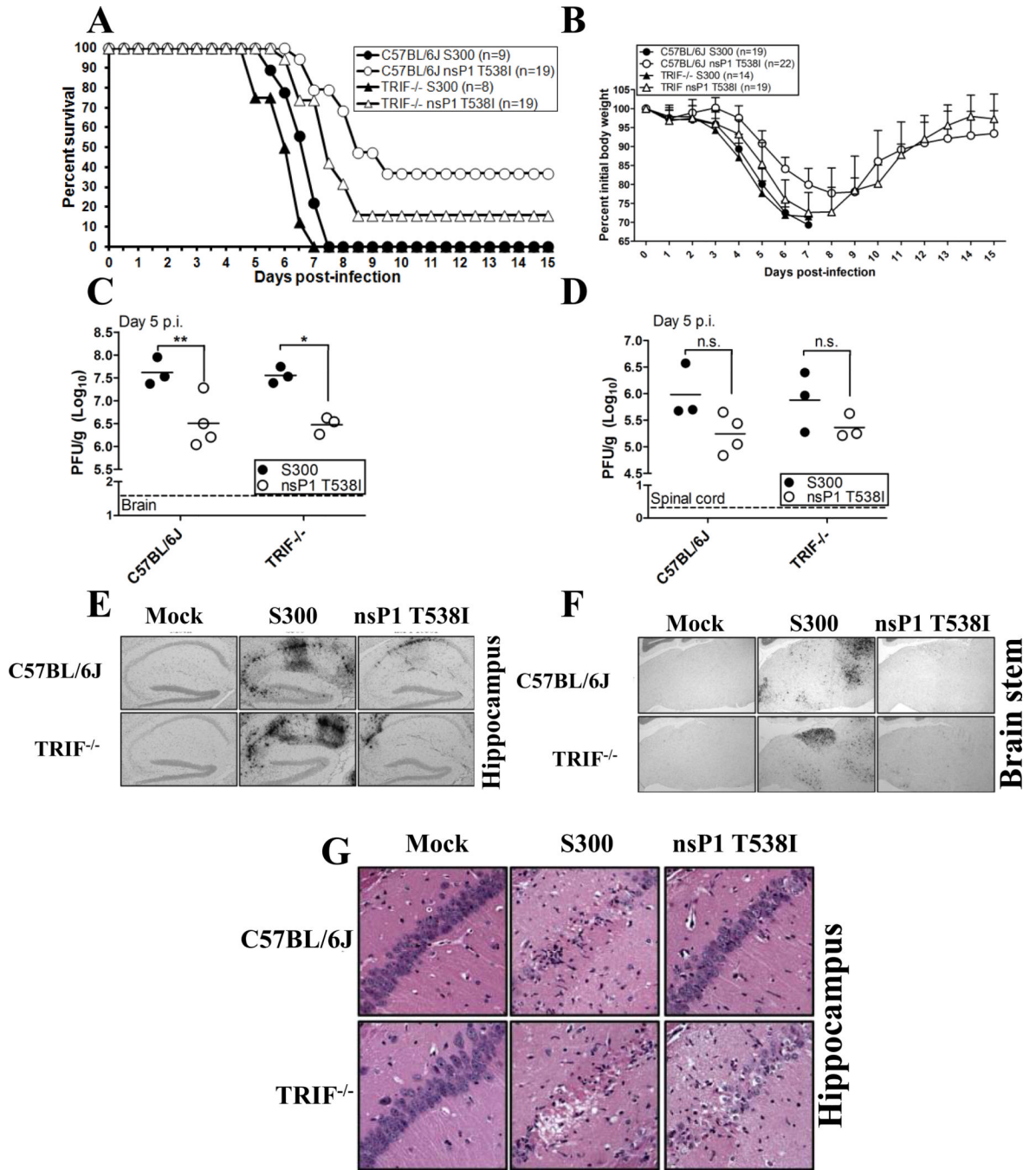
Figure 4. TRIF signaling is not required for viral replication control of nsP1 T538I, but TRIF may play a minor role in protection from SINV-induced disease

Adult 9–12-week-old female C57BL/6J and TRIF^{−/−} mice were infected i.c. with 10^3 PFU of S300 or nsP1 T538I virus. (A) Survival and (B) weight loss of S300 and nsP1 T538I infected C57BL/6J or TRIF^{−/−} mice are shown. The number of mice infected per group is indicated in parentheses. Infectious virus was assayed at 5 days pi within the (C) brain and (D) spinal cord. Titer data are representative of two or more experiments. Asterisks denote $p < 0.05$(*) or $p < 0.01$(**). The dashed line indicates the lower limit of assay sensitivity. Mice were perfused with 15 mL of 4% PFA for *in situ* hybridization and H&E, and brains were paraffin embedded and cut sagitally. Sections were subjected to *in situ* hybridization

with a riboprobe specific for SINV AR86 and shown are (E) hippocampus and (F) spinal cord regions. Nonspecific binding controls included sections from mock-infected mice probed with the AR86 riboprobe, and sections from infected mice probed with a riboprobe specific for Epstein Barr virus (not shown). (G) H&E stained brain sections depicting the hippocampus.
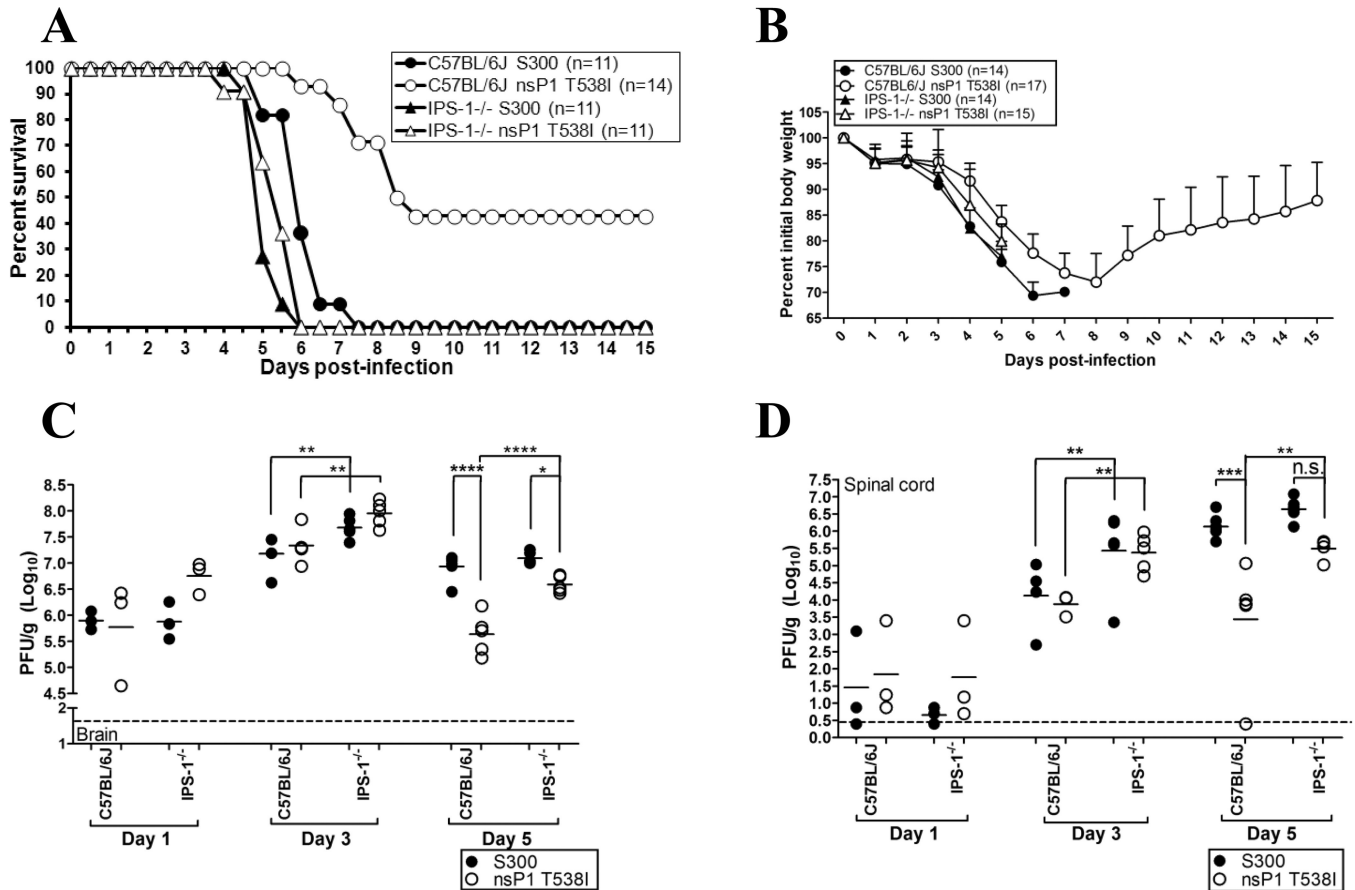
Figure 5. IPS-1 is required for protection from nsP1 T538I and contributes to control of nsP1 T538I

Adult 9–12-week-old female C57BL/6J and IPS-1$^{-/-}$ mice were infected i.c. with 10^3 PFU of S300 or nsP1 T538I virus. Similar (A) survival and (B) weight loss curves between S300 and nsP1 T538I infected IPS-1$^{-/-}$ mice. The number of mice infected per group is indicated in parentheses. Infectious virus was assayed at 1, 3, and 5 days pi in the (C) brain and (D) spinal cord. Titer data are representative of two or more experiments. Asterisks denote $p <$ 0.05(*), $p <$ 0.01(**), $p <$ 0.01(***), and $p <$ 0.0001(****). The dashed line indicates the lower limit of assay sensitivity.
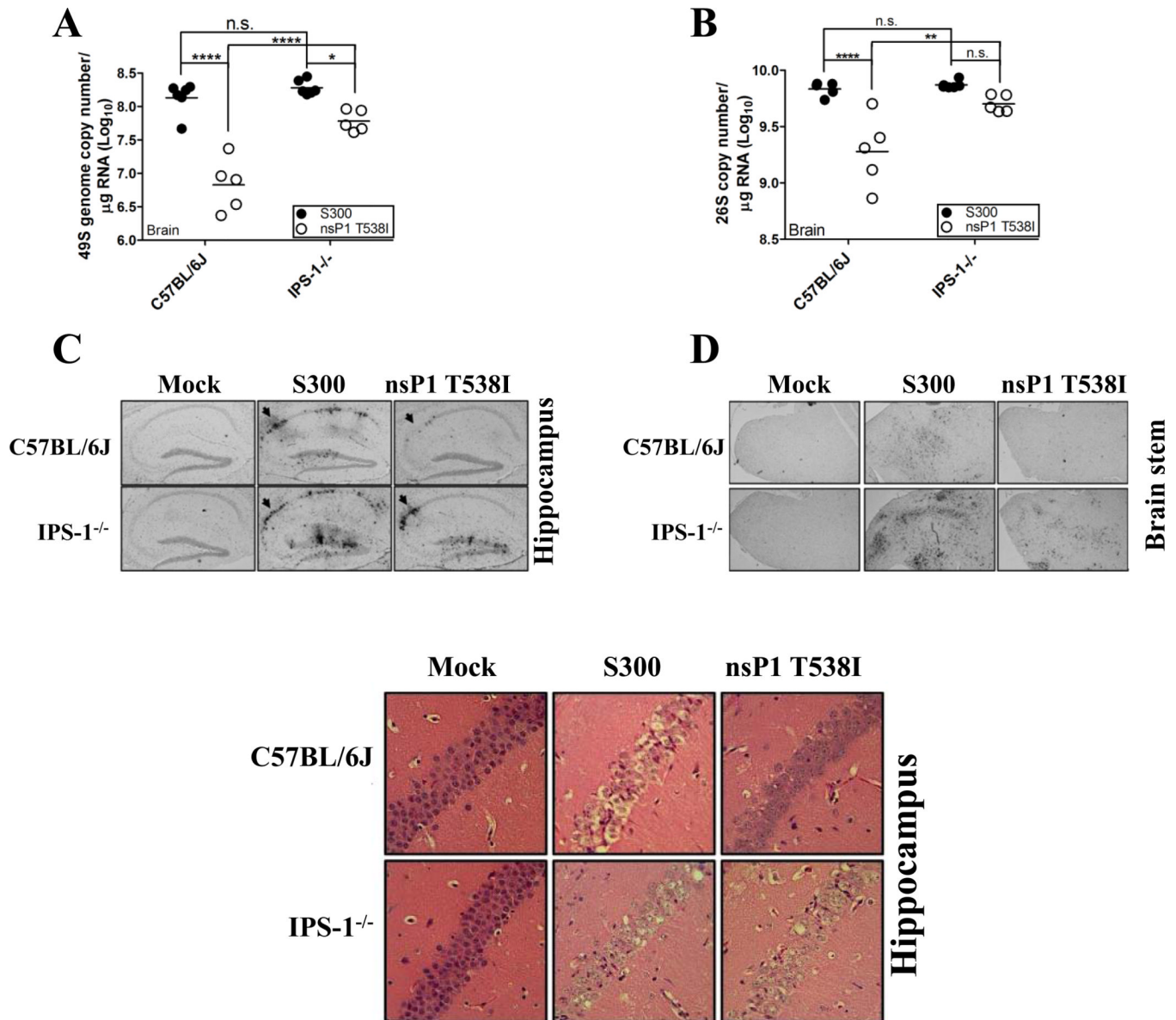
Figure 6. Increased quantity and distribution of viral RNA and neuronal damage in IPS-1$^{-/-}$ mice infected with S300 and nsP1 T538I as compared with C57BL/6 mice infected with nsP1 T538I

C57BL/6J and age-matched IPS-1$^{-/-}$ mice were infected i.c. with 10^3 PFU of S300 or nsP1 T538I virus. Brains were harvested at 5 days pi. (A, B) Mice were perfused with 15 mL of PBS, and RNA was harvested prior to qRT-PCR using primer/probe sets specific for SINV (A) 49S genomic RNA or (B) 26S subgenomic RNA. Asterisks denote $p < 0.05$(*), $p < 0.01$(**), $p < 0.001$(***), or $p < 0.0001$(****). Mice were perfused with 15 mL of 4% PFA for *in situ* hybridization and H&E, and brains were paraffin embedded and cut sagitally. Sections were subjected to (C, D) *in situ* hybridization with a riboprobe specific for SINV AR86 or (E) H&E. Nonspecific binding controls included sections from mock-infected mice probed with the AR86 riboprobe, and sections from infected mice probed with a riboprobe specific for Epstein-Barr virus (not shown). Data shown are representative of three experiments with at least three mice per group.

Table 1

Statistical differences in survival curves within each knockout mouse strain Compared to:

Virus	Mouse Strain	Virus	Mouse Strain	Survival curve Significance
S300	C57BL/6J	S300	IFN-α/βR$^{-/-}$	p<0.0001(****)
S300	C57BL/6J	S300	IPS-1$^{-/-}$	p<0.001(***)
S300	C57BL/6J	S300	MyD88$^{-/-}$	n.s.
S300	C57BL/6J	S300	TRIF$^{-/-}$	p<0.05(*)
nsP1 T538I	C57BL/6J	nsP1 T538I	IFN-α/βR$^{-/-}$	p<0.0001(****)
nsP1 T538I	C57BL/6J	nsP1 T538I	IPS-1$^{-/-}$	p<0.0001(****)
nsP1 T538I	C57BL/6J	nsP1 T538I	MyD88$^{-/-}$	n.s.
nsP1 T538I	C57BL/6J	nsP1 T538I	TRIF$^{-/-}$	n.s.
S300	C57BL/6J	nsP1 T538I	C57BL/6J	p<0.0001(****)
S300	IFN-α/βR$^{-/-}$	nsP1 T538I	IFN-α/βR$^{-/-}$	n.s.
S300	IPS-1$^{-/-}$	nsP1 T538I	IPS-1$^{-/-}$	n.s.
S300	MyD88$^{-/-}$	nsP1 T538I	MyD88$^{-/-}$	p<0.001(***)
S300	TRIF$^{-/-}$	nsP1 T538I	TRIF$^{-/-}$	p<0.0001(****)

Table 2

Percent mortality and mean survival times after i.c. infection with S300 or n

Mouse Strain	Virus	% Mortality	Mean survival time (days)
C57BL/6J[a]	S300	100	6.3
C57BL/6J[a]	nsP1 T538I	62.5	10.7
IFN-α/βR$^{-/-}$	S300	100	3.5
IFN-α/βR$^{-/-}$	nsP1 T538I	100	3.4
IPS-1$^{-/-}$	S300	100	5.1
IPS-1$^{-/-}$	nsP1 T538I	100	5.4
MyD88$^{-/-}$	S300	100	6.2
MyD88$^{-/-}$	nsP1 T538I	75	9.3
TRIF$^{-/-}$	S300	100	5.3
TRIF$^{-/-}$	nsP1 T538I	84.2	8.6

[a]Values are pooled across all experiments.

Table 3

Statistical differences in weight loss on day of peak disease within each I Compared to:

Virus	Mouse Strain	Virus	Mouse Strain	Weight loss Significance
S300	C57BL/6J	S300	IFN-α/βR−/−	$p<0.0001(****)$
S300	C57BL/6J	S300	IPS-1$^{-/-}$	n.s.
S300	C57BL/6J	S300	MyD88$^{-/-}$	n.s.
S300	C57BL/6J	S300	TRIF$^{-/-}$	n.s.
nsP1 T538I	C57BL/6J	nsP1 T538I	IFN-α/βR$^{-/-}$	$p<0.0001(****)$
nsP1 T538I	C57BL/6J	nsP1 T538I	IPS-1$^{-/-}$	n.s.
nsP1 T538I	C57BL/6J	nsP1 T538I	MyD88$^{-/-}$	n.s.
nsP1 T538I	C57BL/6J	nsP1 T538I	TRIF$^{-/-}$	$p<0.01(**)$
S300	C57BL/6J	nsP1 T538I	C57BL/6J	$p<0.001(***)$
S300	IFN-α/βR$^{-/-}$	nsP1 T538I	IFN-α/βR$^{-/-}$	n.s.
S300	IPS-1$^{-/-}$	nsP1 T538I	IPS-1$^{-/-}$	$p<0.0001(****)$
S300	MyD88$^{-/-}$	nsP1 T538I	MyD88$^{-/-}$	$p<0.0001(***)$
S300	TRIF$^{-/-}$	nsP1 T538I	TRIF$^{-/-}$	n.s.